Journal of Inflammation Research

Dovepress
Taylor & Francis Group

Open Access Full Text Article

ORIGINAL RESEARCH

Usp18 Mediates D-Dopachrome Tautomerase-Induced Astrocytic Inflammation After Spinal Cord Injury

Xingyuan Zhang[1,*], Yuxuan Hou[1,*], Rixin Cai[1], Yue Zhou[1], Bingqiang He[1], Zhilong Cao[1,2], Aicheng Li[1], Honghua Song[1], Yingjie Wang[1], Haiyan Jiang[3], Lei Qi[4], Yongjun Wang[1,5]

[1]Key Laboratory of Neuroregeneration of Jiangsu and Ministry of Education, Co-innovation Center of Neuroregeneration, Nantong University, Nantong, 226001, People's Republic of China; [2]Department of Intensive Care Unit, Nantong Third People's Hospital, Nantong, 226001, People's Republic of China; [3]Health Management Center, Affiliated Hospital of Nantong University, Nantong, 226001, People's Republic of China; [4]Department of Emergency Medicine, Affiliated Hospital of Nantong University, Nantong, 226001, People's Republic of China; [5]Department of Burn and Plastic Surgery, Affiliated Hospital of Nantong University, Nantong, 226001, People's Republic of China

*These authors contributed equally to this work

Correspondence: Lei Qi, Department of Emergency Medicine, Affiliated Hospital of Nantong University, Nantong, 226001, People's Republic of China, Email qilei723@ntu.edu.cn; Yongjun Wang, Key Laboratory of Neuroregeneration, Nantong University, 19 Qixiu Road, Nantong, 226001, People's Republic of China, Tel + 86-513-85051818, Fax +86-513-85511585, Email wyjbs@ntu.edu.cn

Background: D-dopachrome tautomerase (D-DT), a homolog of macrophage migration inhibitory factor (MIF), has been revealed to promote astrocytic inflammation and worsen neuropathology following spinal cord injury (SCI). So far, the mechanism about D-DT-activated astrocytic inflammation remains elusive. Ubiquitin-specific peptidase 18 (Usp18) is an active player in regulating innate immunity through ISG15-deconjugated dependent or independent manner in multiple cell types. Whether D-DT activates astrocytic inflammation *via* regulation of Usp18 deserves further study.

Methods: SCI model was prepared by cord contusion at T8-T10 of rats. The expression changes of D-DT and Usp18 were examined by ELISA, Western blot, RT-PCR or immunohistochemistry. Primary astrocytes were treated by different concentration of D-DT, either for transcriptome sequencing or for analysis of D-DT-mediated expression of Usp18. Knockdown of CD74 or Usp18 expression was performed by siRNA transfection of astrocytes. The locomotor functions were assessed using the Basso, Beattie, and Bresnahan (BBB) locomotor scale.

Results: Usp18 was significantly upregulated in the astrocytes at lesion sites following SCI, in parallel with the elevation of D-DT protein levels. D-DT inhibitor 4-CPPC remarkably decreased the astrocytic expression of USP18. Transcriptome sequencing of D-DT-stimulated primary astrocytes identified that Usp18 was the hub modulator of D-DT-mediated astrocytic inflammation. D-DT-mediated expression of Usp18 was able to activate MAPKs, contributing to the production of proinflammatory cytokines and chemokines. Specifically, phosphorylation of P38 kinase was shown to promote the expression of Usp18 by formation of a positive feedback loop. Administration of D-DT inhibitor 4-CPPC at lesion sites following SCI significantly reduced the protein levels of Usp18 and ameliorated functional deficits of rat hindlimb locomotion.

Conclusion: SCI-induced elevation of D-DT at lesion sites activates astrocytic inflammation *via* upregulating the expression of Usp18. Identification of this novel regulator associated with astrocytic inflammation will provide an alternative target for clinical therapy of neuroinflammation.

Keywords: D-DT, Usp18, astrocyte, inflammation, ubiquitination, spinal cord

Introduction

Spinal cord injury (SCI) often causes a devastating physical consequence that is difficult to be efficiently repaired.[1,2] Following initial insults to the spinal cord, the secondary tissue damage will immediately proceeds, characterized by a series of biochemical and cellular events that exacerbate neurological deficits.[3,4] Excessive neuroinflammation evoked by damage-

Received: 20 November 2024
Accepted: 17 May 2025
Published: 11 June 2025

associated molecular patterns (DAMPs) and infiltrating leukocytes is shown to be responsible for neuropathological progression following SCI.[5,6] The overproduced DAMPs, either actively secreted by immune cells or passively released from necrotic cells at lesion site, elicit inflammatory responses of immune cells and glial cells through interaction with pattern recognition receptors (PRRs). These PRRs include Toll-like receptors (TLRs), Nod-like receptors (NLRs), RIG-like receptors (RLRs), AIM2-like receptors (ALRs) and C-type lectin receptors, which are broadly expressed by most cells in the spinal cord. Reactive astrocytes, which undergo morphological and functional changes, have been shown to express PRRs profile similar to those of microglia. Thereby, they serve as active players in mediating neuroinflammation under pathological conditions.[7–11] Reversible ubiquitin modification has been revealed to regulate astrocytic reaction including gliosis and inflammatory responses following various extracellular stimuli.[12,13] Particularly, nuclear factor kappa-B (NFκB), the key proinflammatory transcription factor of astrocytes,[14,15] is susceptible to be regulated by reversible ubiquitination of its upstream factors, such as TAK1, TRAF6 or RIPK1.[16–18] As such, ubiquitination-mediated signaling may represent the repertoire expansion of the regulatory mechanisms on astrocytic inflammation. Notably, the astrocytes lack several essential factors for transduction of inflammatory signals in immune-regulating cells, such as the receptor-interacting protein (RIP), which is only specifically expressed in inflammatory cells and oligodendrocytes.[19] Conceivably, the astrocytes can contribute to neuroinflammation in alternative regulatory mechanisms following SCI.

Ubiquitin-specific peptidase 18 (Usp18) is a deubiquitinase also known as UBP43. It is initially identified as the only protease that specifically deconjugates interferon-stimulated gene product 15 (ISG15), an ubiquitin-like protein, from the substrate proteins (deISGylation).[20] Analogous to ubiquitination, protein modification via ISG15 results in alteration of protein stability, thereby affects cellular biological processes including innate immunity and antiviral responses.[21–25] In addition, Usp18 can act as a negative modulator of type I IFN signaling by binding the interferon-alpha/beta receptor (IFNAR2), irrespective of its catalytic activity.[26] Increasing evidence shows that Usp18 is actually a multifaceted protein implicating in diverse pathophysiological roles, including muscle differentiation, innate immunity and tumor progression.[18,27–30] Intriguingly, the exact functions of Usp18 in neurological disorders remain controversial. For example, T cell-derived Usp18 favors for the EAE pathogenesis,[31] while clinical investigation demonstrates that Usp18 deficiency correlates with microgliopathies and higher MS severity.[32,33] Moreover, Usp18 plays active roles in reactive astrogliosis associating with functional deterioration following SCI,[34] but it also performs to protect spinal cord against ischemia/reperfusion injury.[35] So far, the neuropathological function of Usp18 and the underlying mechanisms have not been fully elucidated.

Expression of Usp18 in immune cells is markedly induced by type I and type III IFNs, LPS, TNF-α or polyI:C in response to infectious or inflammatory challenges.[36–41] Less is known, however, whether the DAMPs are able to regulate expression of Usp18 for the activation of innate immunity following SCI. D-dopachrome tautomerase (D-DT) belongs to macrophage migration inhibitory factor (MIF) family, also known as MIF-2.[42] It shares not only structural similarity, but also the overlapping receptor and biological function with MIF.[43] D-DT is detected in most tissues including heart, liver, brain, spinal cord, spleen, lung, skeletal muscle, kidney and testes.[9] Its aberrant expression contributes to inflammatory activation, ischemic injury of heart, wound healing and tumorigenesis.[44–47] An inducible release of D-DT has been observed from neurons and astrocytes, rather than from microglia or oligodendrocytes to elicit inflammation following SCI.[9] Similar to MIF, D-DT is recognized as an active DAMP with prominent neuropathological feature.[9,10] Mechanistically, D-DT triggers signal transduction mainly through interaction with CD74 receptor, causing the activation of the intracellular mitogen-activated protein kinase (MAPK) and p65NFκB translocation into nucleus.[9,48,49] Given the impacts of Usp18 on NFκB signaling in inflammatory activation of multiple cell types,[31,50,51] the deubiquitinase is therefore assumed to be associated with regulating D-DT-mediated astrocytic inflammation following SCI. In the present study, the distinct function of Usp18 in regulating D-DT-induced astrocytic inflammation following rat SCI was identified. The results have provided new clues for clinical therapy of neuroinflammation following CNS insults.

Materials and Methods

Animals

Adult male Sprague-Dawley (SD) rats, weighing 180–220 g, were provided by the Center of Experimental Animals, Nantong University. All animal experiments were approved by *the Animal Care and Use Committee of Nantong University (License No. SYXK (Su) 2020–0029)* and were in accordance with *the Guidelines for the Care and Use of Laboratory Animals developed by the National Institutes of Health, USA*. All subjects were housed in standard cages (five rats in each cage) in an environment maintained at 22±2°C on a 12–12 h light-dark cycle and had free access to water and food.

Establishment of Rat SCI Model and Drug Treatment

The number of animals subjected to surgery was calculated by six per experimental group in triplicate. The SCI model of rat was prepared by contusion as was previously described.[52] All subjects were anesthetized by intraperitoneal injection with 10% compound anesthetic at 0.4 mL/100g body weight. The fur around the surgical site was shaved and the skin was disinfected with iodophor, followed by an exposure of the 8th to 10th thoracic vertebra with a scalpel. A laminectomy was performed at the ninth thoracic vertebral level (T9) with the intact dura. The dorsal spinal processes T7 and T11 were fixed with the clamps of the impactor device (IH-0400 Impactor, Precision Systems and Instrumentation). The impactor rod was positioned centrally at T9 (about 3 mm in length) over the midline of the spinal cord, and the contusion was carried out by receiving a 160-kilodyne impact. After removing the rod, the wound was immediately irrigated. The modeling was evaluated by visual check of hematoma formation and paralysis of the hind limbs after animal awakening from the anesthesia. For drug delivery, a total of 8 μL of 100 mm D-DT inhibitor 4-CPPC (AOBIOUS) was intrathecally injected prior to the incision suture. The rats were subsequently subcutaneously administered with a prophylactic dose of enrofloxacin (Sigma-Aldrich; 1 mg/kg) once a day for 7 consecutive days in order to preventing urinary tract against infection. Manual expression of bladders was performed twice a day until the animals recovered the spontaneous voiding.

Cell Culture and Treatment

Primary astrocytes were prepared from the spinal cord of newborn SD rats, 1–2 days after birth according to the previous description.[53] Briefly, the spinal cords were dissected out and placed into 0.01M PBS containing 1% penicillin-streptomycin. The cord capsule was stripped off, followed by mincing with scissors and digestion with 0.25% trypsin for 15 min at 37 °C. The digestion was terminated by addition of Dulbecco's Modified Eagle's Medium (DMEM) - high glucose medium containing 10% fetal bovine serum (FBS), 1% penicillin-streptomycin and 1% L-glutamine. The suspension was then centrifuged at 1200 rpm for 5 min, and the cells were resuspended and seeded onto poly-L-lysine pre-coated culture flask in the presence of 5% CO_2. The medium was changed every 3 days until the whole flask was fully covered with cells. After 7–9 days, the culture flask was shaken at 250 rpm overnight to remove non-astrocytes. Astrocytic phenotype was evaluated by characteristic morphology and by immunostaining of glial fibrillary acid protein (GFAP) antibody. Astrocytes with purity more than 95% were acceptable for the respective experiments.

To examine the effects of D-DT on the expression of Usp18, the primary astrocytes were treated with various selective inhibitor SB203580 (TOCRIS), SP600125 (TOCRIS) or PD98059 (TOCRIS) in the presence or absence of 1 μg/mL recombinant D-DT (Aviva Systems Biology) for 24 h prior to biochemical assay.

For siRNA knockdown of CD74 expression in the astrocytes, the cells were transfected with CD74 siRNA3 (5'- TGA ACT ACC CAC AGC TGA A −3') or scramble siRNA (5'-GC AUA GGC UUU UCU AGA GCC dTdT-3') with iMAX transfection reagent (Invitrogen) for 24 h. The same method was applied to interfere with Usp18 expression of astrocytes using Usp18 siRNA1 (5'- TCA GAC ATG TTG CCT TAA C −3'). The astrocytes were then incubated at medium in the absence of 1% penicillin-streptomycin for 24 h, followed by stimulation with 1 μg/mL D-DT recombinant protein for another 24 h before ELISA or Western blot assay.

Wound Healing Assay

The primary astrocytes were seeded into a 6-well plate and grown to confluent monolayers. The cells were then starved in DMEM supplemented with 0.15 mg/mL of mitomycin C (Sigma, USA) for 12 h, followed by scratching to generate a 2-mm wound. Subsequently, the cells were incubated at 0–2.5 μg/mL D-DT and allowed for a culture for 48 h. Closure of the wound was monitored and photographed. Representative images were captured and analyzed with Wimscratch Quantitative Wound Healing Image Analysis (Wimasis GmbH, Munich, Germany).

Cell Proliferation Assay

The primary astrocytes were suspended in the fresh prewarmed culture medium and plated at a density of 1×10^5 cells/mL in a 96-well plate precoated with 0.01% poly-L-lysine. After addition of D-DT recombinant protein, 50 mm of EdU was added to the culture, and the cells were incubated for an additional 2 h. Next, Hoechst33342 was applied to counterstain the cell nucleus for 10–20 min. The cells were subsequently fixed with 4% formaldehyde in PBS for 30 min, followed by an assay using Cell-Light EdU DNA Cell Proliferation Kit according to the manufacturer's protocol. Cell proliferation (ratio of EdU^+ to all cells) was analyzed under a DMR fluorescence microscope (Leica Microsystems, Bensheim, Germany). The assays were repeated in triplicate.

Western Blot

Protein was extracted from cells with a buffer containing 50 mm Tris (pH 7.4), 150 mm NaCl, 1% Triton X-100, 1% sodium deoxycholate, 0.1% SDS and 1 mm PMSF, after the cell treatment with D-DT recombinant protein or various inhibitors for 24 h. Alternatively, protein was extracted from the spinal segments (1 cm) at injured site at 0d, 1d, 4d and 1w following contusion (n = 6). Samples were vortexed for 30 min and centrifuged at 12000 rpm for 15 min. The supernatants were collected and stored at −20 °C for use. Protein concentration of each sample was measured by the BCA method to maintain the same loads according to the manufacturer's instructions. Proteins were heated at 95 °C for 5 min, and 20 μg of each sample was electrophoretically separated on 10% SDS-PAGE gel, followed by transferring onto a polyvinylidene difluoride (PVDF) membrane. The membrane was blocked with 5% skim milk in Tris-buffered saline containing 0.1% Tween-20 for 1 h, and then an overnight incubation at 4 °C with primary antibodies: D-DT (1:500, Abcam); p65NFκB (1:1000, CST); ERK (1:1000, CST); p-ERK (1:1000, CST); JNK (1:1000, CST); p-JNK (1:1000, CST); P38 (1:1000, CST); p-P38 (1:1000, CST); GFAP (1:1000, CST); STAT3 (1:1000, CST); pSTAT3 (1:1000, CST). After washing 3 times with TBST for 10 min each, the membrane was incubated with secondary antibody goat-anti-mouse HRP or goat-anti-rabbit HRP (1:1000, Beyotime) for 2 h at room temperature. The HRP activity was detected using an ECL kit. The image was scanned with a GS800 Densitometer Scanner (Bio-Rad), and the data were analyzed using PDQuest 7.2.0 software (Bio-Rad). The β-actin (1:5000) or GAPDH (1:5000) was used as the internal control.

ELISA

Cells or tissue samples were sonicated using the lysis buffer supplemented with a protease inhibitor PMSF as mentioned above. Homogenates were centrifuged at 12,000 rpm for 15 min at 4 °C, and the supernatants were collected for TNF-α, IL-1β, CCL2, CCL5 (MULTI SCIENCES) and D-DT (LMAI) ELISA assay. The concentration of the cytokines was expressed as pg/mL for the supernatant, while pg/mg for the lysate of the cells or the cord tissues. Plates were read with a multifunctional enzyme marker (Biotek Synergy2) at a 450 nm, 570 nm or 630 nm wavelength according to the protocol.

Tissue Immunofluorescence

The subjects were intraperitoneally anesthetized at 0 d, 1 d, 4 d and 7 d following SCI and drug administration. Then, they were transcardially perfused with 0.01 M PBS (pH 7.4) and 4% paraformaldehyde. The vertebra segments were harvested from six experimental subjects of each time point, post-fixed with 4% paraformaldehyde in PBS at 4°C overnight. After being equilibrated in 10%, 20% and 30% sucrose for gradient dehydration, they were sectioned on

a cryostat at a thickness of 12 μm, beginning from 0.25 cm length to the lesion epicenter. The sections were blocked with 0.01 M PBS containing 3% BSA, 0.1% Triton X-100 and 10% normal goat serum for 1 h at 37 °C, and incubated overnight at 4 °C with primary antibodies: GFAP (1:400, Sigma); Usp18 (1:200, Abcam). Thereafter, the sections were rinsed with PBS and incubated with the Cy3-labeled goat anti-rabbit IgG (1:400, Proteintech) or the Alexa Fluor 488-labeled donkey anti-mouse IgG (1:400, Abcam). Sections were observed under a fluorescence microscope (ZEISS, axio image M2).

Transcriptome Sequencing

Total RNAs of astrocytes following treatment with 1.0 μg/mL recombinant D-DT for 12 h, 24 and 48 h respectively, were extracted using the mirVana miRNA Isolation Kit (Ambion, Austin, TX) according to the manufacturer's instructions. They were then selected by RNA Purification Beads (Illumina, San Diego, CA), and undergone library construction and RNA-seq analysis. The library was constructed by the Illumina TruSeq RNA sample Prep Kit v2 and sequenced by the Illumina HiSeq-2000 for 50 cycles. High-quality reads that passed the Illumina quality filters were kept for the sequence analysis.

Bioinformatics Analysis

Differentially expressed genes (DEGs) were designated in a criterion of greater or less than twofold changes in comparison with the control. Function of genes was annotated by Blastx against the NCBI database or the AGRIS database with E value threshold of 10^{-5}. Gene ontology (GO) classification was obtained by WEGO via GO id annotated by Perl and R program. Kyoto Encyclopedia of Genes and Genomes (KEGG) pathways were assigned to the sequences using KEGG Automatic Annotation Server (KAAS) online. For all heatmaps, genes were clustered by Jensen-Shannon divergence.

A reconstructed gene network was created using the Ingenuity Pathway Analysis (IPA) Software on the basis of DEGs to investigate their regulatory pathways and cellular functions.

Polymerase Chain Reaction (PCR)

Total RNAs were extracted with Trizol (Sigma) from cells transfected with CD74 or USP18 siRNA (Ribobio) using a LipofectamineTM RNAiMAX transfection reagent (Invitrogen) for 24 h. Fluorescence-tagged control Cy3 was used as a marker for evaluation of transfection efficiency. The first-strand cDNA was synthesized using HiScript II Q RT SuperMix for qPCR (+gDNA wiper) (Vazyme) in a 20 μL reaction system, and diluted at 1:3 before used in assays. The sequence-specific primers were designed and synthesized by Ribobio. Primer pairs for *cd74*: forward primer 5'-GAC CCG TGA ACT ACC CAC AG-3', reverse primer 5'-CCA GTG GCT CTT TAG GTG GA-3'; for *GAPDH*, forward primer 5'-GGG TCC CAG CTT AGG TTC AT-3', reverse primer 5'-GAG GTC AAT GAA GGG GTC GT-3'; for *Usp18*, forward primer 5'- AGG GTC CTT TCT GGC TTG TG −3', reverse primer 5'- GGG TCC TTT CTG GCT TGT GT −3'. Reactions were performed in a final volume of 10 μL (1 μL cDNA template and 9 μL reaction buffer containing 5 μL of 2 × ChamQ Universal SYBR qPCR Master Mix, 3 μL of RNase free ddH_2O, and 0.5 μL of anti-sense and sense primers each). Reactions were processed using one initial denaturation cycle at 94°C for 5 min, followed by 40 cycles of 94°C for 30 sec, 60°C for 30 sec and 72°C for 30 sec. Fluorescence was recorded during each annealing step. At the end of each PCR run, data were automatically analyzed by the system and amplification plots were obtained. The expression levels were normalized to an endogenous *GAPDH*. The relative expression was then processed using the $2^{-\Delta\Delta CT}$ method. In addition, a negative control without the first-strand cDNA was also performed.

Behavioral Tests

The hindlimb locomotor function was evaluated using the Basso, Beattie and Bresnahan (BBB) locomotor scale as previously described.[54] Briefly, after intrathecal injection of 8 μL of 100 mm vehicle or 4-CPPC at 0d, 7d, 14d and 21d, three well-trained investigators blind to the study were invited to observe the behavior of the subjects for 5 min. The BBB score ranged from 0 (no hindlimb movement) to 21 (normal movements, coordinated gait with parallel paw placement) according to the rating scale. Scores from 0 to 7 indicated the return of isolated movements in the hip, knee

and ankle joints. Scores from 8 to 13 meant the return of paw placement and coordinated movements with the forelimbs. Scores from 14 to 21 indicated the return of toe clearance during stepping, predominant paw position, trunk stability and tail position. The tests were independently scored by the investigators following assessments.

Statistical Analysis

Statistical analysis used GraphPad Prism 8 software (San Diego, CA, USA). All data were presented as means ± SEM. The sample size of six animals per group is based on power analysis in GPower software, and the parameter is set to alpha < 0.05 and Power (1-β) = 0.80. Comparisons between two groups following a normal distribution were analyzed by two-tailed unpaired Student's *t* test or the Mann–Whitney test when the distribution was not parametric. Differences between multiple groups were analyzed using one-way or two-way analysis of variance (ANOVA), followed by Tukey's or Sidak's post hoc test. P value < 0.05 was considered statistically significant and was denoted in the figures as $p < 0.05$.

Results

Usp18 is Significantly Upregulated in the Astrocytes at Lesion Sites Following SCI

To examine the correlations between D-DT and Usp18 expression at lesion sites following SCI, the protein levels of D-DT and Usp18 were determined from 1 cm cord segments at lesion sites at 0d, 1d, 4d and 7d, respectively. Western blot or ELISA assay revealed that the expression of both Usp18 and D-DT was synchronously upregulated from 1 d onwards following SCI (Figure 1a–c). As astrocytes constitutively express CD74 membrane receptor relevant to D-DT-mediated neuroinflammation,[9,10] the expression changes of Usp18 within GFAP-positive astrocytes before or after SCI were thus detected by immunostaining. The results demonstrated that expression of astrocytic Usp18 was remarkably induced at 1d, 4d and 7d (Figure 1d). However, administration of 8 μL of 100 mm D-DT inhibitor 4-CPPC at lesion sites significantly suppressed those increases (Figure 2a–p). The data indicate that SCI-induced D-DT elevation may contribute to promoting astrocytic expression of Usp18.

Transcriptome Sequencing Reveals That Astrocytic Expression of Usp18 is Induced by D-DT

To validate the promoting role of D-DT on the astrocytic expression of Usp18, the primary astrocytes were stimulated with 1.0 μg/mL recombinant rat D-DT protein (rD-DT) for 12 h, 24 and 48 h, respectively, followed by transcriptome sequencing. GO (gene ontology) annotation of differentially expressed genes (DEGs) demonstrated that the rD-DT mediates an array of biological processes of astrocytes including wound healing, response to proinflammatory cytokines, angiogenesis and migration of leukocytes (Figure 3a). KEGG enrichment revealed that TNF-α and NFκB signaling were activated by the rD-DT (Figure 3a). Heatmap and cluster dendrogram were constructed using inflammation-related DEGs at 3 time points, showing dynamical changes of these genes in response to rD-DT challenge (Figure 3b). Gene network was created with ingenuity pathway analysis (IPA) using the DEGs integrated from different time points, highlighting that Usp18 was the prominent regulator of rD-DT-activated signaling in astrocytes (Figure 3c). The data indicate that D-DT is able to induce astrocytic expression of Usp18.

D-DT Promotes Astrocytic Expression of Usp18 Through CD74 Receptor

To further clarify the regulatory role of D-DT/CD74 axis on astrocytic expression of Usp18, the primary astrocytes with purity over 92% were stimulated with 0–2.5 μg/mL rD-DT for 24 h (Figure 4a). Western blot demonstrated that the protein levels of astrocytic Usp18 were markedly elevated in rD-DT concentration-dependent manner (Figure 4b). As D-DT is shown to activate intracellular signaling through interaction with CD74 receptor, siRNA transfection was then applied to interfere with the CD74 expression of astrocytes. The CD74 siRNA3 with the highest interference efficiency was selected out of three siRNAs (Figure 4c). Following transfection of the astrocytes with CD74 siRNA3 for 48 h, prior to treatment with 1 μg/mL rD-DT for 24 h, Usp18 expression in the cells was found to be significantly reduced at both translational and transcriptional levels in comparison with the scramble (Figure 4d and e). The data indicate that D-DT promotes astrocytic expression of Usp18 through CD74 receptor.

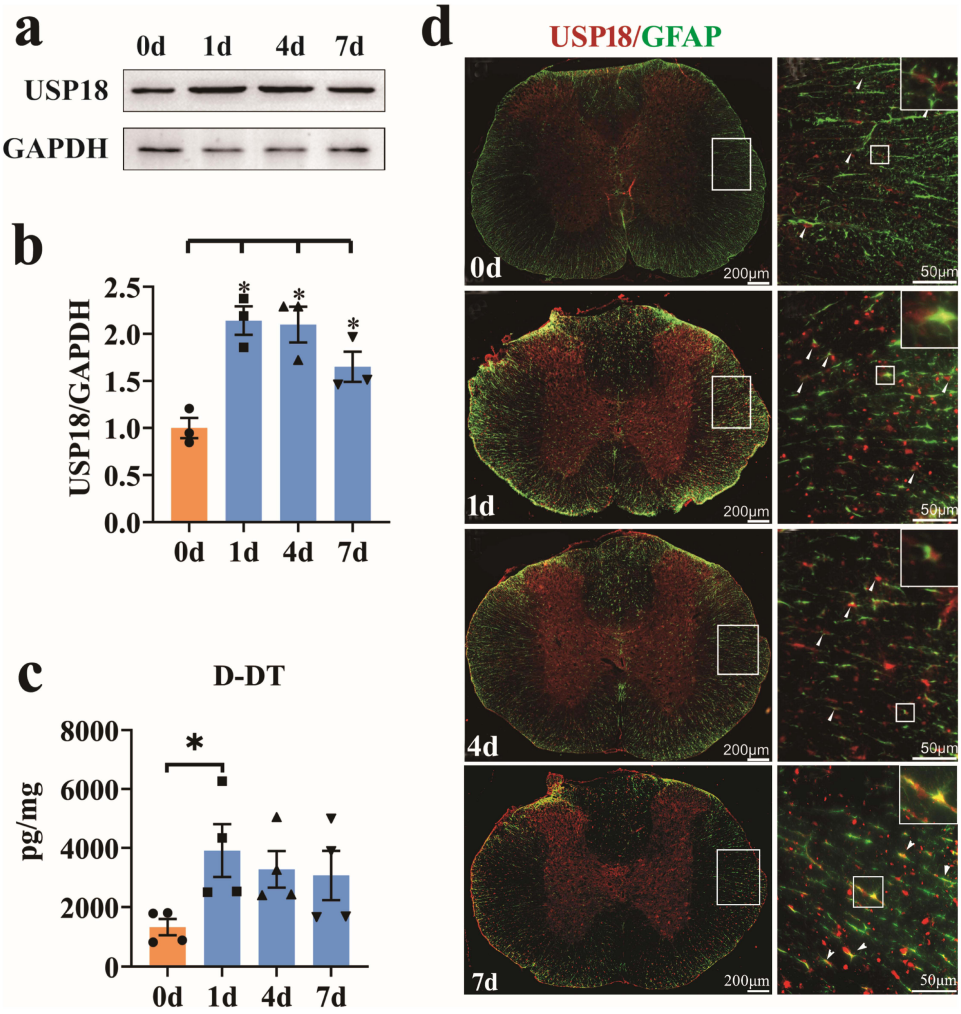

Figure 1 Expression analysis of D-DT and Usp18 in the injured spinal cord of rats. (**a**) Western blot analysis of Usp18 protein at lesion site of the cord at 0, 1, 4 and 7 days following SCI, n = 3. Quantities were normalized to endogenous GAPDH. (**b**) Quantification data as shown in (**a**) (*P < 0.05). (**c**) ELISA measurement of D-DT expression at 0, 1, 4 and 7 days following SCI. Experiments were performed at least in technical triplicates. Error bars represent the SEM (*P < 0.05). (**d**) Colocalization analysis of Usp18 with GFAP-positive astrocytes after SCI. The sections were prepared using a cryostat from 0.25 cm length to the lesion epicenter. Rectangle indicates region magnified. Arrowheads indicate the positive signals. Scale bars, 200 μm, and 50 μm in magnification.

D-DT-Induced Astrocytic Expression of Usp18 Functions on Activation of Intracellular MAPKs

To ascertain the effects of D-DT-mediated Usp18 expression on the activation of MAPKs and production of proinflammatory cytokines, the primary astrocytes were incubated at 1 μg/mL rD-DT for 24h with or without siRNA knockdown of Usp18. The Usp18 siRNA1 was chosen for its highest interference efficiency. The results revealed that rD-DT was able to increase phosphorylated levels of ERK, JNK and P38 (Figure 5a–c). However, siRNA knockdown of Usp18 resulted in a significant decrease of these phosphorylated kinases, together with downstream p65NFκB in comparison with the scramble (Figure 5d–f). Accordingly, cytokines IL-1β and CCL2, rather than TNF-α or CCL5, were markedly induced by D-DT/Usp18 axis (Figure 6a–d). The data indicate that D-DT-induced Usp18 functions on activation of MAPKs-mediated inflammatory responses of astrocytes.

Usp18 Promotes P38 Activation of Astrocytes with a Positive Feedback

To shed light on the possible roles of MAPKs on the regulation of Usp18, the primary astrocytes were treated with the selective inhibitor of ERK (PD98059), JNK (SP600125) or P38 (SB203580) to examine the expression changes of Usp18. The results showed that addition of 10 μM P38 inhibitor SB203580, rather than that of ERK (PD98059) or JNK

https://doi.org/10.2147/JIR.S505433

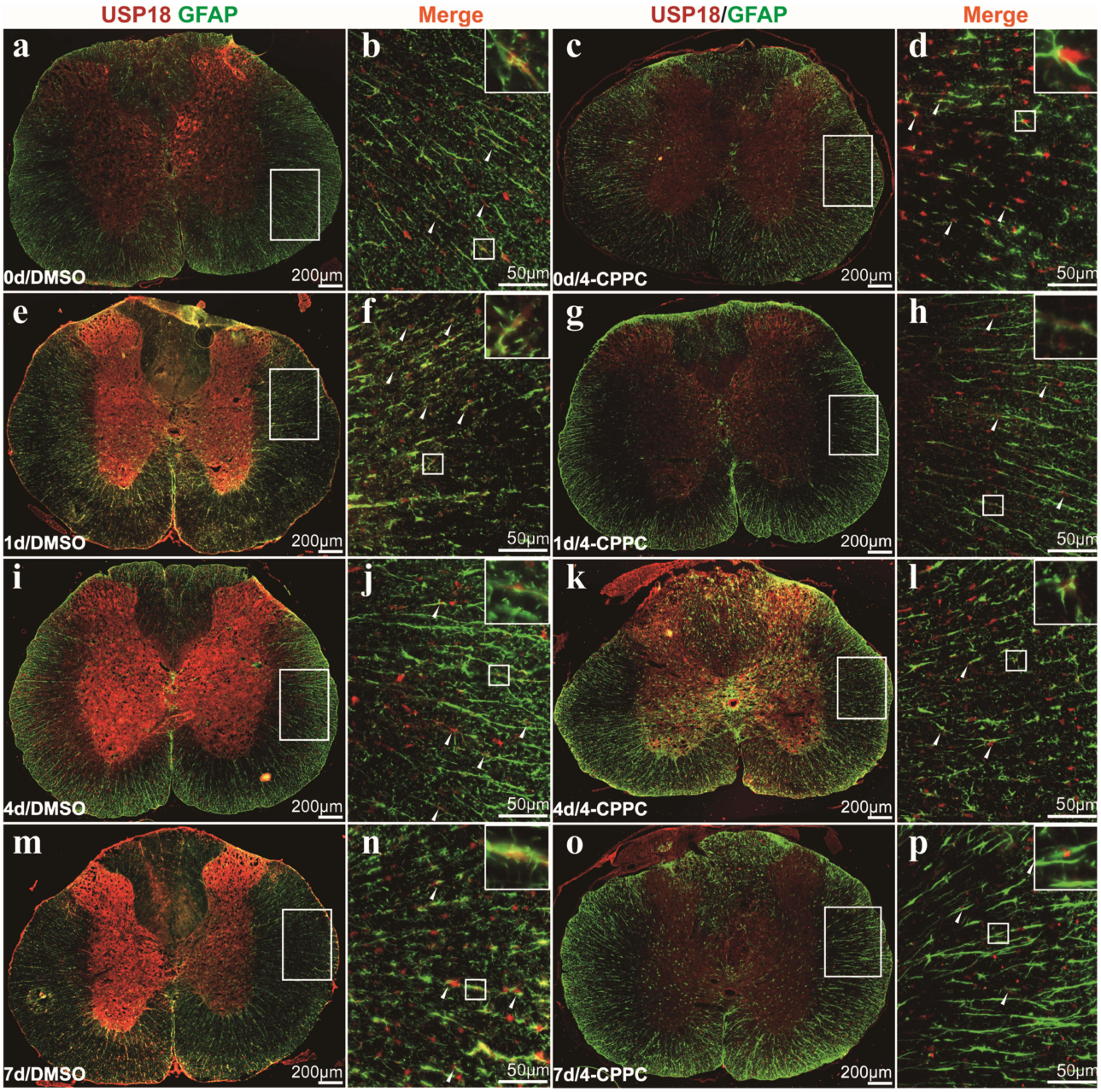

Figure 2 Colocalization analysis of Usp18 with GFAP-positive astrocytes by immunostaining following SCI at 0, 1, 4 and 7d, with or without injection of 8 μL of 100 mm 4-CPPC (**a–p**), respectively. Rectangle indicates region magnified. Arrowheads indicate the positive signals. Scale bars, 200 μm, and 50 μm in magnification.

(SP600125) in the presence of 1 μg/mL rD-DT for 24 h, was able to inhibit the Usp18 expression at translational and transcriptional levels (Figure 7a–c). Taken together, the data indicate that D-DT can promote astrocytic Usp18 expression by forming a positive feedback loop with MAPKs.

Usp18 Makes No Impact on D-DT-Mediated Astrocytic Migration

Astrocytes will undergo a phenotypic change known as reactive astrogliosis in relation to neuropathological progress following SCI,[55] and both GFAP and phosphorylated STAT3 are the hallmarks of reactive astrocytes.[56] To understand the roles of Usp18 in the D-DT-mediated astrocytic events, the cells were subsequently stimulated with 1 μg/mL rD-DT for

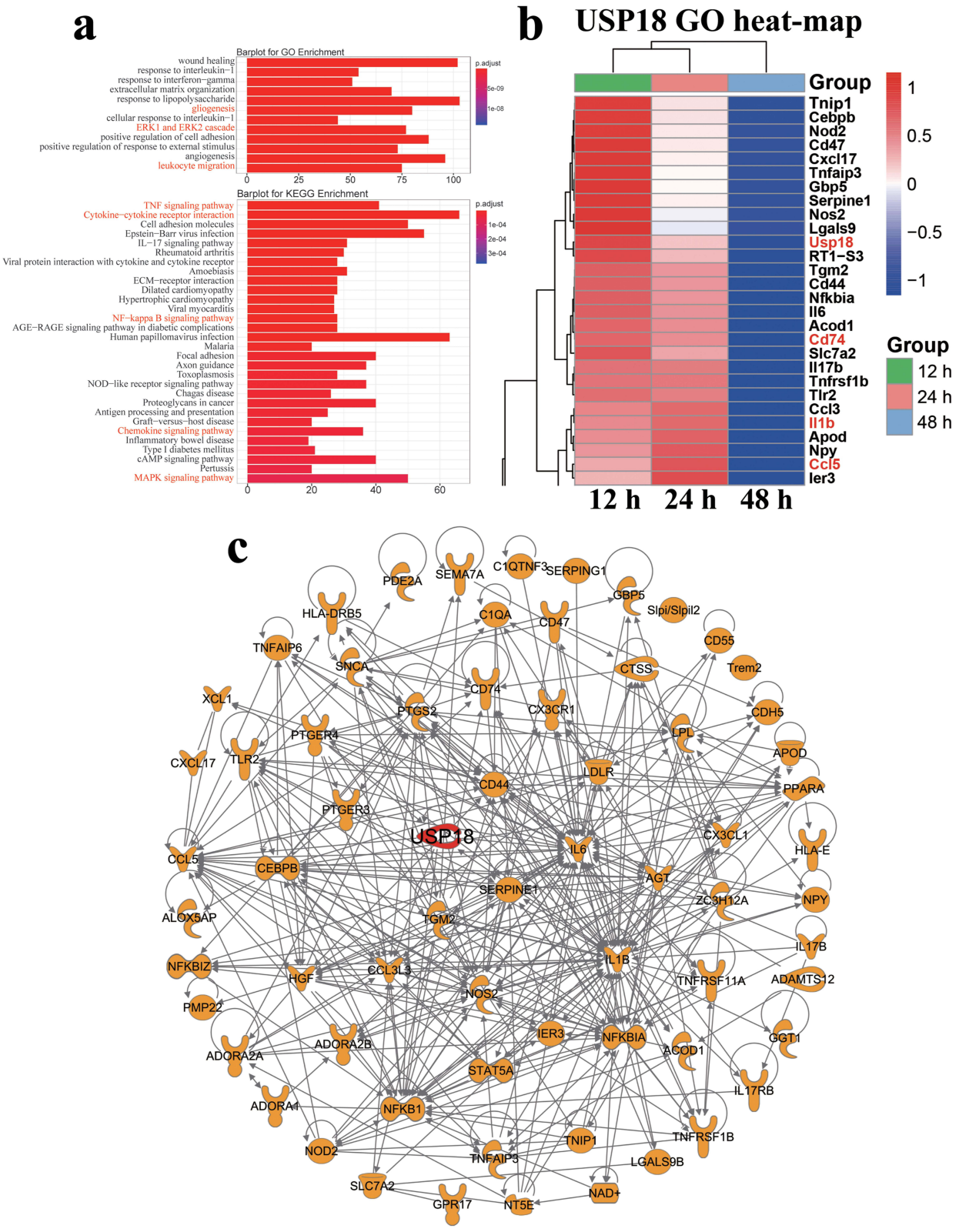

Figure 3 Functional annotation and expression profiling of DEGs following stimulation of astrocytes with 1.0 μg/mL rD-DT for 12 h, 24 and 48 h. (**a**) GO analysis and KEGG enrichment of the DEGs. (**b**) Heatmap and cluster dendrogram of integrated DEGs at 3 time points. The color scale illustrates the relative expression level of the indicated genes across all samples: red denotes expression > 0 and blue denotes expression < 0. (**c**) A gene network was created using the IPA on the basis of integrated DEGs at 3 time points.

https://doi.org/10.2147/JIR.S505433

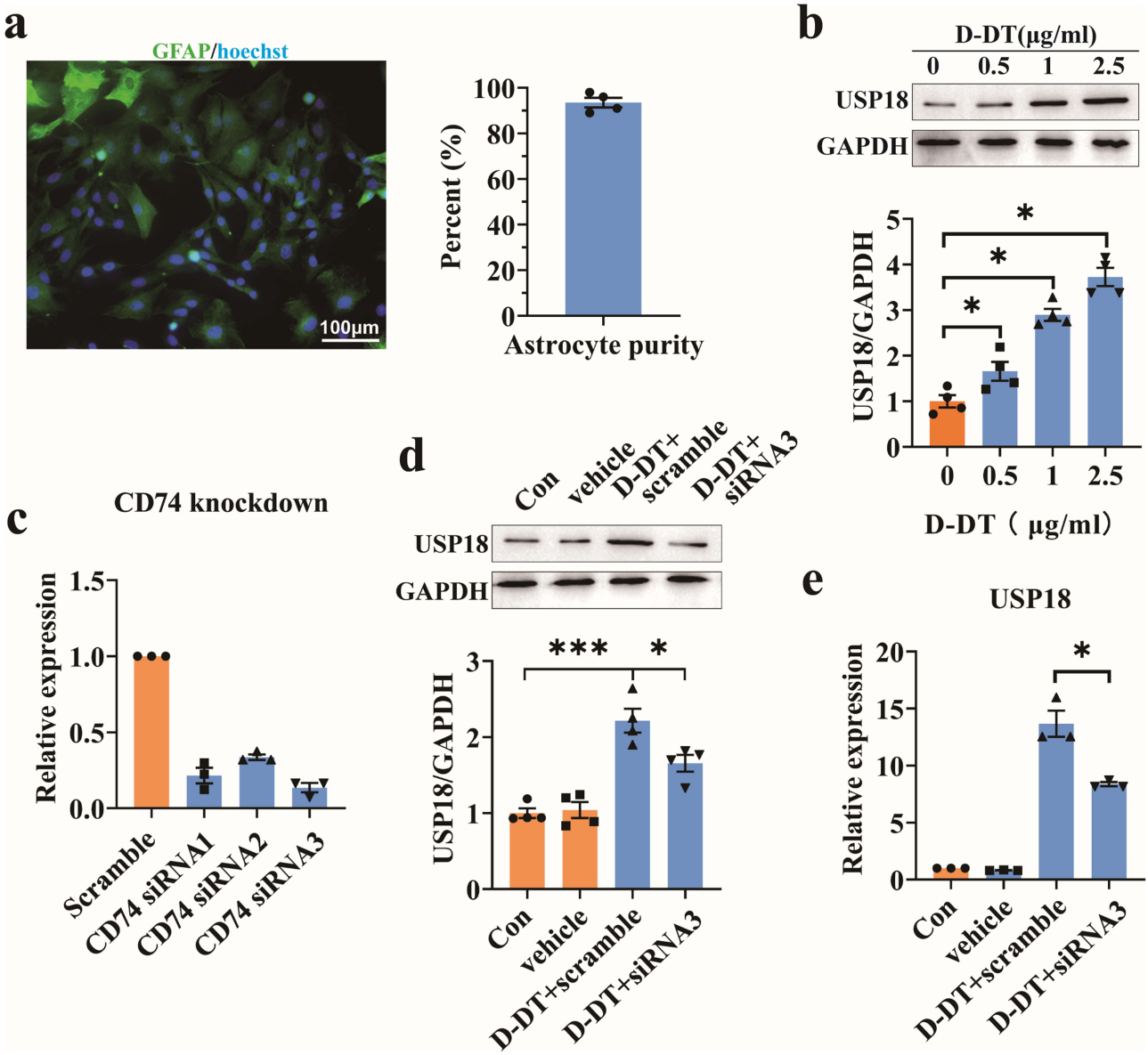

Figure 4 D-DT promotes astrocytic expression of Usp18 through CD74 receptor. (**a**) Primary cultured rat spinal cord astrocytes stained with GFAP and Hoechst 33342 with purity over 92%. (**b**) Western blot analysis of Usp18 in the astrocytes stimulated by 0–2.5 μg/mL rD-DT for 24h. Quantities were normalized to endogenous GAPDH. *P < 0.05. (**c**) Interference efficiency of siRNA oligonucleotides for CD74 was measured by RT-PCR, and siRNA3 was used for the knockdown experiments. (**d**) Western blot analysis of Usp18 in the astrocytes following CD74 knockdown for 48h prior to treatment of the astrocytes with 1 μg/mL rD-DT for 24h. Scramble was used as control. Quantities were normalized to endogenous GAPDH. *P < 0.05; ***P < 0.001). (**e**) RT-PCR analysis of Usp18 expression in the astrocytes with the same treatment as those of Western blot. Experiments were performed in triplicates. Error bars represent the SEM (*P < 0.05). Scale bars, 100 μm.

24 h with or without interference of Usp18 for 48 h. Western blot showed that D-DT/Usp18 signaling has undetectable effects on the astrocyte reactivity (Figure 8a–c). Also, they did not affect proliferation of astrocytes, as was determined by EdU assay after stimulation of the cells with 0–2.5 μg/mL rD-DT for 24 h with or without siRNA knockdown of Usp18 (Figure 8d–g). Wound scratch assay demonstrated that, however, the rD-DT at 0.5–2.5 μg/mL was efficient in promoting astrocytic migration at 48 h in comparison with the control, whereas transfection of Usp18 siRNA did not affect such events (Figure 8h–k). The data indicate that Usp18 has no impact on D-DT-mediated astrocytic migration following SCI.

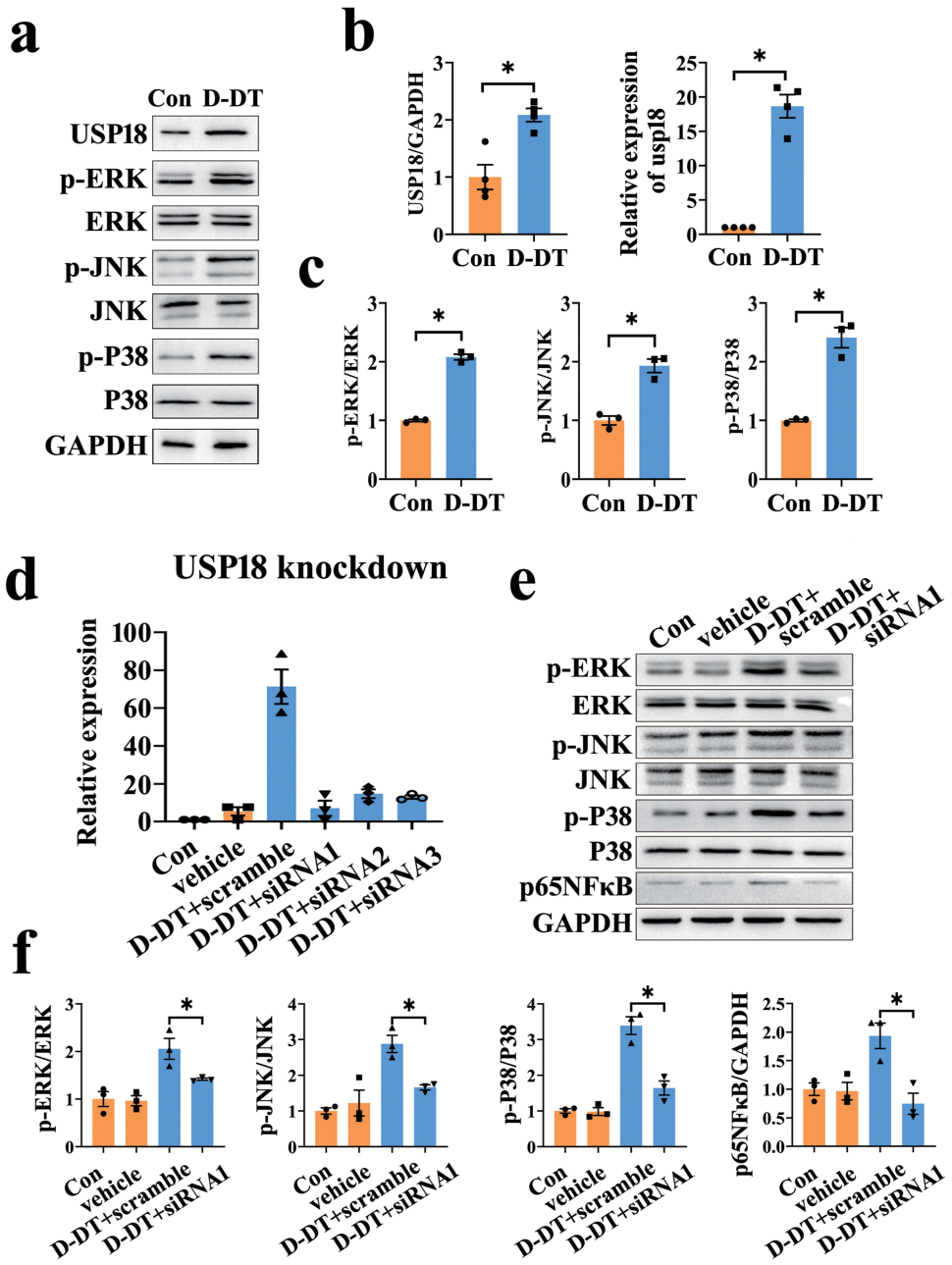

Figure 5 Knockdown of Usp18 attenuates D-DT-mediated activation of MAPKs in the astrocytes. (**a**) Western blot analysis of Usp18 and phosphorylated MAPKs in the astrocytes stimulated by 1 μg/mL rD-DT for 24h. Quantities were normalized to endogenous GAPDH. (**b**) Quantification data as shown in (**a**) and RT-PCR analysis of Usp18 expression in the astrocytes with the same treatment. *P < 0.05. (**c**) Quantification data of phosphorylated MAPKs as shown in (**a**). *P < 0.05. (**d**) Interference efficiency of siRNA oligonucleotides for Usp18 was measured by RT-PCR, and siRNA1 was used for the knockdown experiments. (**e**) Western blot analysis of phosphorylated MAPKs and NFκB in the astrocytes following Usp18 knockdown for 48h prior to treatment of the astrocytes with 1 μg/mL rD-DT for 24h. Scramble and vehicle were used as control. Quantities were normalized to endogenous GAPDH. (**f**) Quantification data as shown in (**e**). Experiments were performed in triplicates. Error bars represent the SEM (*P < 0.05).

Administration of D-DT Selective Inhibitor Downregulates Astrocytic Expression of Usp18 and Improves Hindlimb Locomotor Function Following Rat SCI

Now that Usp18 plays critical roles in D-DT-mediated neuropathology following SCI, D-DT selective inhibitor 4-CPPC was thus used to evaluate its effects on the astrocytic Usp18 expression, as well as the hindlimb locomotor function. A total of 8 μL of 100 mm 4-CPPC or vehicle was intrathecally injected at the lesion sites of the cords following SCI. Western blot demonstrated that the protein levels of Usp18 was significantly attenuated by 4-CPPC treatment at 1d, 4d and 7d (Figure 9a and b).

https://doi.org/10.2147/JIR.S505433

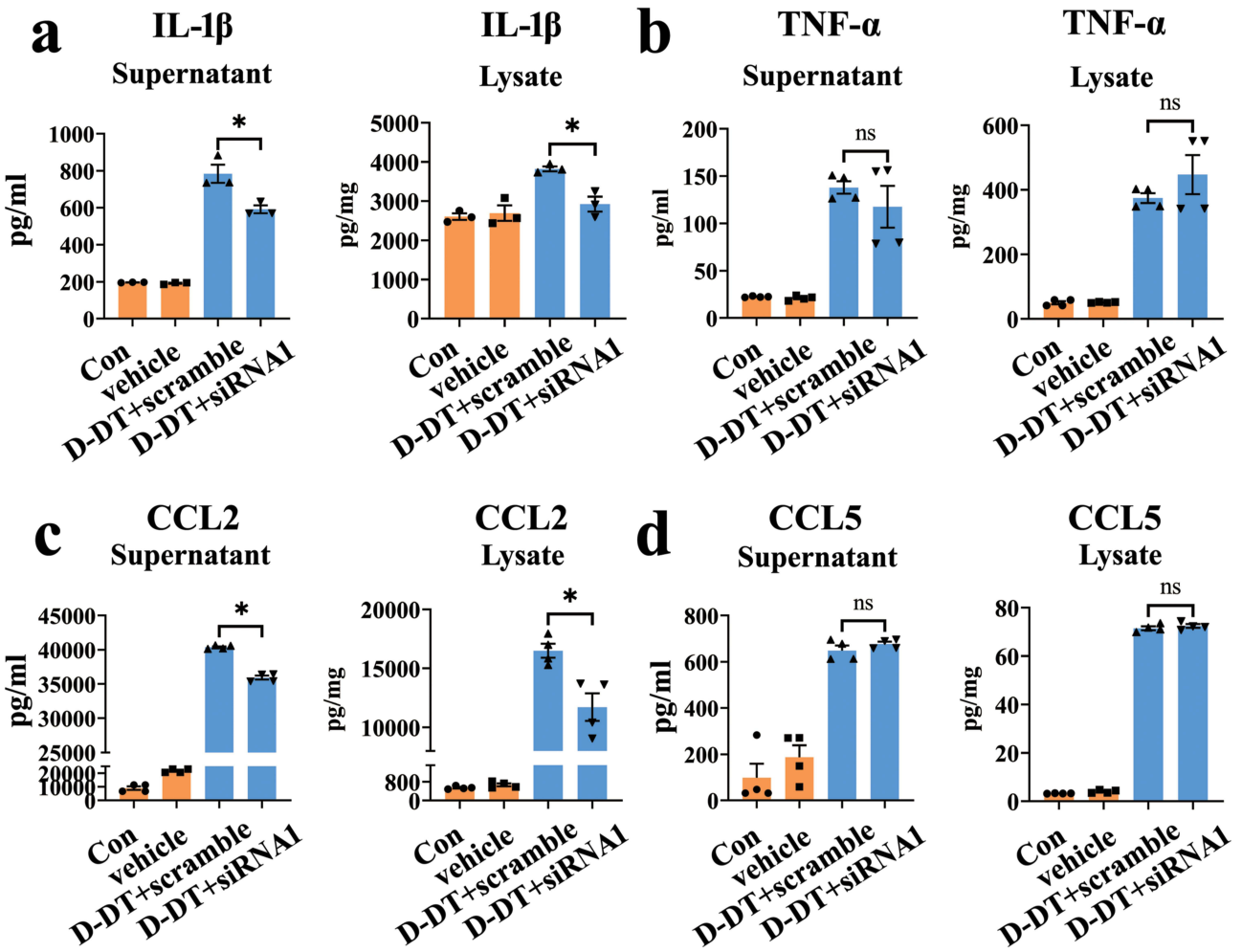

Figure 6 Effects of Usp18 interference on the D-DT-induced production of proinflammatory mediators from astrocytes. ELISA assays of IL-1β (**a**), TNF-α (**b**), CCL2 (**c**) and CCL5 (**d**) in the astrocytes following Usp18 knockdown for 48h prior to treatment of the astrocytes with 1 μg/mL rD-DT for 24h. Scramble and vehicle were used as control. Experiments were performed at least in triplicates. Error bars represent the SEM. (**a**),*P < 0.05; (**c**),*P < 0.05.

Accordingly, the expression of Usp18 in the astrocytes also decreased (Figure 2). Behavioral tests by BBB scores within 3 weeks showed that administration of 4-CPPC remarkably favors for the recovery of rat hindlimb locomotor function after SCI (Figure 9c). The data indicate that interference of D-DT/Usp18 axis following SCI is beneficial for improvement of hindlimb locomotor function.

Discussion

D-DT is a homolog of MIF with 34% sequence identity in humans and 27% in mice at the protein levels.[47] Several studies demonstrate that D-DT participates in catalytic and immune functions, as well as tumor growth and metastasis.[43,57,58] In the damaged spinal cord, D-DT is induced to serve as activator of neuroinflammation, contributing to locomotor function impairment.[9,10] These pathological roles partially overlap with those of MIF. For example, MIF has also been shown to be induced by thrombin following SCI, and activates some proinflammatory mediators including CCL2 and CCL5.[53,59,60] Distinctively, DDT lacks the CXXC redox and pseudo (E)LR motifs present in MIF, which are essential for sensing redox signals by thiol-based regulators or interaction with CXCR2.[49,61] D-DT also has fewer post-translational modifications than those of MIF.[43,62,63] As a consequence, D-DT may exhibit some unique or even opposite pathophysiological roles. Typical evidence displays that expression of D-DT negatively, while MIF positively correlates with obesity.[64,65] Mechanistically, D-DT activates intracellular signals through interaction with CD74 receptor with or without cooperation of CD44 co-receptor, dependent on cell types,[49,64] while the MAPKs and NFκB are the important

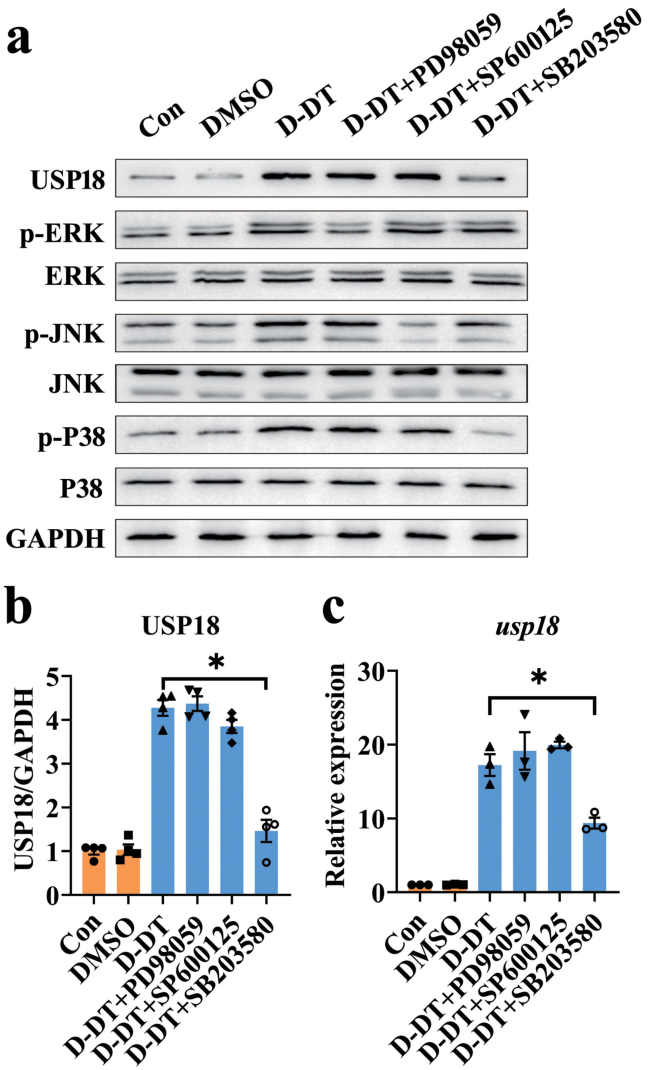

Figure 7 Determination of Usp18 expression in the astrocytes following treatment with MAPKs inhibitors. (**a**) Western blot analysis of protein levels of phosphorylated ERK, JNK, P38 kinase and Usp18 after astrocyte treatment with 10 μM P38 (SB203580), ERK (PD98059) or JNK (SP600125) inhibitor in the presence of 1 μg/mL rD-DT for 24h. Quantities were normalized to endogenous GAPDH. (**b**) Quantification data as shown in (**a**). Error bars represent the SEM (*P < 0.05). (**c**) RT-PCR analysis of Usp18 expression in the astrocytes with the same treatment. Experiments were performed at least in triplicates. Error bars represent the SEM (*P < 0.05).

effectors of D-DT/CD74 axis.[49] In the present study, the rat SCI model was used to examine the regulatory mechanism of D-DT-mediated neuroinflammation, due to its similar pathological characterization to human, such as the formation of glial scar and cystic cavity. We unveiled that a positive feedback loop comprised of Usp18 and MAPKs was responsible for D-DT-activated astrocytic inflammation, suggesting a novel regulatory mechanism of D-DT in mediating neuropathology.

Astrocytes can mount diverse responses associating with pathogenesis and tissue repair in the context of CNS insults.[66] Multiple signal pathways mediate the reactivity of astrocytes, in which MAPKs/NFκB has been defined as a primary player in response to various stimuli.[14,67] Some regulators are able to fine-tune the pathological functions of reactive astrocytes through crosstalk with MAPK/NFκB. For example, interaction of STAT3 with NFκB performs to synergistically regulate target genes, whereas that of the aryl hydrocarbon receptor (AHR) can inhibit NFκB activity in the mouse astrocytes.[68,69] Several deubiquitinating enzymes are shown active in the astrocyte reaction by activation of NFκB in experimental autoimmune encephalomyelitis (EAE) disease.[70] These suggest that various

https://doi.org/10.2147/JIR.S505433

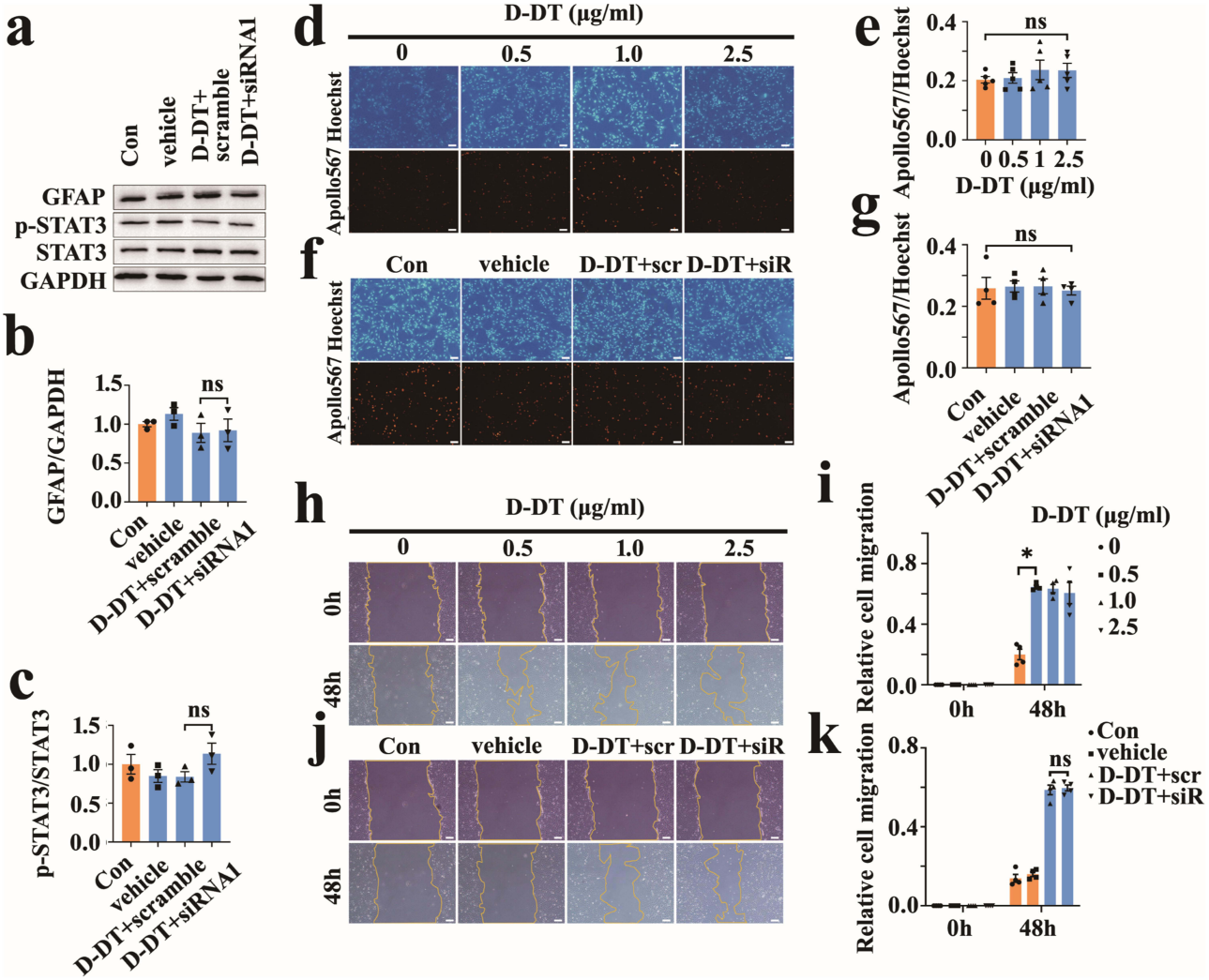

Figure 8 Effects of Usp18 on the D-DT-induced cell proliferation and migration of astrocytes. (**a**) Western blot analysis of GFAP following Usp18 knockdown of astrocytes for 48h prior to treatment with 1 μg/mL rD-DT for 24h. Quantities were normalized to endogenous GAPDH.(b, c) Quantification data as shown in (a). (d–g) EdU assay of astrocyte proliferation after cell treatment with 0–2.5 μg/mL rD-DT for 24h (d and e), or Usp18 knockdown for 48h prior to treatment with 1 μg/mL rD-DT for 24h (f and g). (h–k) Wound scratch assay of astrocyte migration after treatment with 0–2.5 μg/mL rD-DT for 24h (h and i), or Usp18 knockdown for 48h prior to treatment with 1 μg/mL rD-DT for 24h (j and k). Scramble and vehicle were used as control. Experiments were performed at least in triplicates. Error bars represent the SEM (*P < 0.05). Scale bars, 50 μm.

roles of reactive astrocytes are closely related to the crosstalk of multiple signaling pathways. Here, Usp18 was revealed to regulate D-DT-mediated IL-1β and CCL2, rather than TNF-α and CCL5 in the astrocytes, possibly attributing to the interwoven signal pathways.

As a deubiquitinating enzyme, Usp18 has been identified in multiple tissues to perform various physiological and pathological functions including anti-apoptosis and innate immunity modulation.[71,72] By removing ISG15 from substrate proteins,[37] Usp18-mediated functions are mostly associated with the deISGylation of ISG15 in the many cell types. But Usp18-regulated innate immunity appears to be ISG15 independent.[73] In hepatocytes, stimuli of TNF-α or LPS result in upregulation of Usp18 expression, but a remarkable inhibition of IFN signaling. This in turn worsens ischemia/reperfusion injury.[38] In the CNS, however, Usp18 competes with JAK1 for binding to the IFNAR2, thus restrains activation of microglia in the white matter.[33] Also, Usp18 can deubiquitinate the TAK1-TAB1 complex.[31] This modification not only mediates autoimmune diseases by inhibiting NFκB and NFAT activation in the T cells, but also activates inflammatory responses of immune-competent cells through regulation of MAPKs, as TAK1 is an upstream component of the MAPKs cascade. All these suggest that Usp18 represents a critical mediator of innate and adaptive

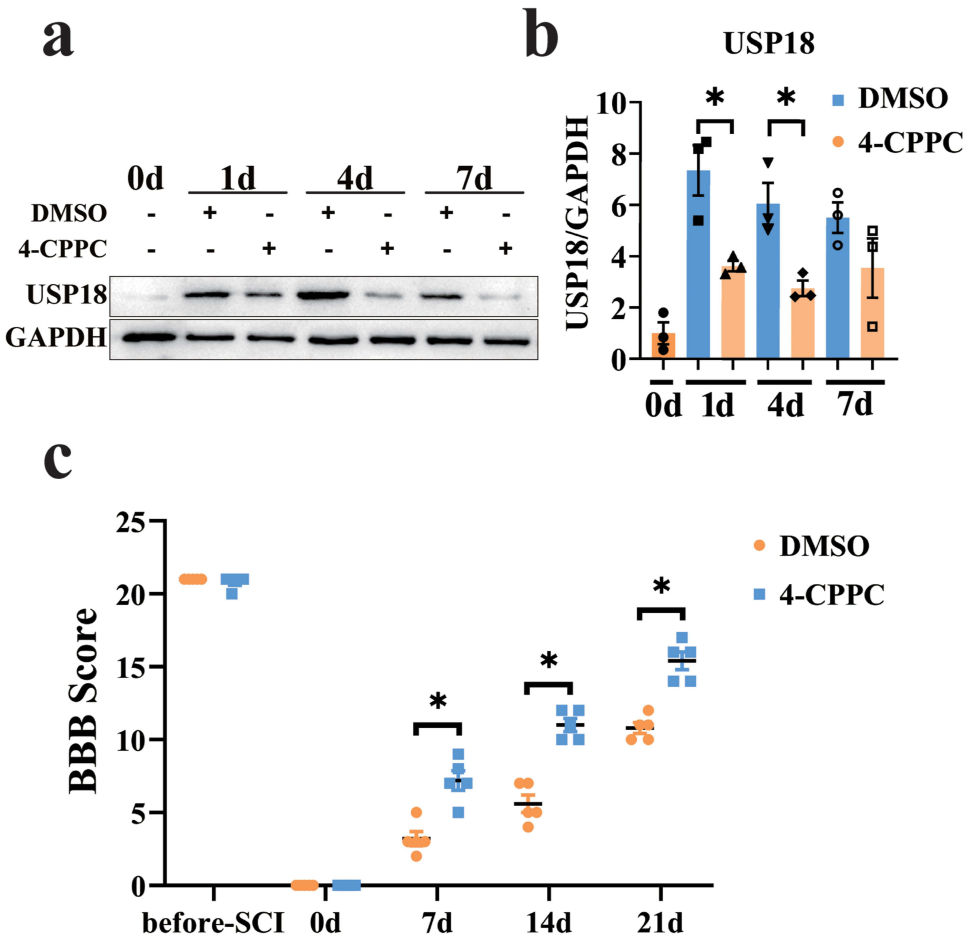

Figure 9 Effects of D-DT inhibition on the expression of Usp18 and locomotor functional recovery following rat SCI. (**a**) Western blot analysis of Usp18 from 1 cm segments following injection of 8 μL of 100 mm 4-CPPC or vehicle at lesion sites of spinal cord at 0, 1, 4, and 7d, respectively. (**b**) Quantification data as shown in (**a**). Quantities were normalized to endogenous GAPDH. Experiments were performed in triplicates. Error bars represent the SEM, *P < 0.05, two-way ANOVA with Tukey's test. (**c**) BBB score of hindlimbs locomotor function at 0d, 7d, 14d and 21d following intrathecal injection of 4-CPPC or vehicle at lesion sites. Error bars represent the SEM, *P < 0.05, two-way ANOVA followed by Sidak's post hoc test.

immunity. In the present study, we elucidated that Usp18 was required for D-DT-mediated inflammatory response of astrocytes through activation of MAPKs, similar to those of Usp12 in LPS-induced macrophage responses.[74] These imply a conserved mechanism of Usp18 in regulating innate immunity in different cell types, providing a promising therapeutic target for neuroinflammation and the consequent tissue damage.

Although D-DT has been shown to be involved in activating the astrocytic inflammation following SCI, it has undetectable effects on astrocyte reactivity, as was examined by GFAP hallmarker. Knockdown of astrocytic Usp18 expression also did not affect D-DT-mediated cell events, aside from cell migration. However, the deubiquitinating enzyme has been shown to promote reactive astrogliosis by stabilizing SOX9 following SCI.[34] The controversial results may come from differences in astrocyte reaction under regulation of interwoven signal pathways in response to complex stimuli in vivo.

In conclusion, as illustrated in Figure 10, SCI results in elevation of D-DT protein at lesion sites, which functions to activate astrocytic inflammation through promoting the expression of Usp18. Usp18 is essential for activation of MAPKs and forms a positive feedback loop with P38, thereby regulates the expression of proinflammatory mediators. The findings have provided a potential target for clinical therapy of neuroinflammation.

https://doi.org/10.2147/JIR.S505433

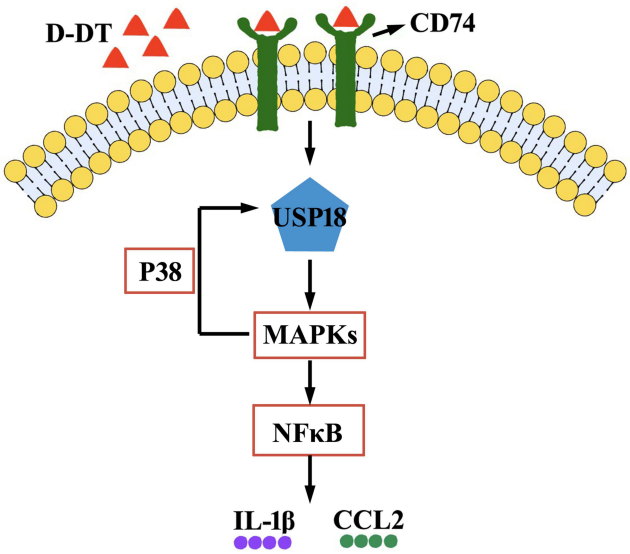

Figure 10 Illustration of D-DT-induced Usp18 involved in the activation of astrocytic inflammation.

Abbreviations

ANOVA, Analysis of variance; CNS, Central nervous system; D-DT, D-dopachrome tautomerase; MIF, Macrophage migration inhibitory factor; DAMP, Damage-associated molecular pattern; USP18, Ubiquitin-like protease 18; NFκB, Nuclear factor kappa-B; PBS, Phosphate buffered saline; MAPK, Mitogen-activated protein kinases; SCI, Spinal cord injury; GFAP, Glial fibrillary acid protein; KEGG, Kyoto Encyclopedia of Genes and Genomes; IPA, Ingenuity Pathway Analysis; Q-PCR, Quantitative real-time PCR; BBB assessment, Basso, Beattie, and Bresnahan assessment; ELISA, Enzyme-linked immunosorbent assay.

Data Sharing Statement

The datasets used and/or analyzed during the current study are available from the corresponding author on reasonable request.

Ethics Approval and Consent to Participate

All animal experiments were approved by the *Animal Care and Use Committee of Nantong University and the Jiangsu Province Animal Care Ethics Committee*.

Acknowledgments

No additional acknowledgements.

Author Contributions

All authors made a significant contribution to the work reported, whether that is in the conception, study design, execution, acquisition of data, analysis and interpretation, or in all these areas; took part in drafting, revising or critically reviewing the article; gave final approval of the version to be published; have agreed on the journal to which the article has been submitted; and agree to be accountable for all aspects of the work.

Funding

This study was supported by the National Natural Science Foundation of China (No. 32471191), the Jiangsu Planned Projects for Postdoctoral Research Fund (2021K031A), the Deputy General Manager Project of Science and Technology of Jiangsu Province (FZ20210652), and the Science and Technology Program of Nantong (JC2023047).

Disclosure

The authors have declared that no competing interests exist.

References

1. O'Shea TM, Burda JE, Sofroniew MV. Cell biology of spinal cord injury and repair. *J Clin Invest*. 2017;127:3259–3270. doi:10.1172/JCI90608
2. Ahuja CS, Wilson JR, Nori S, et al. Traumatic spinal cord injury. *Nat Rev Dis Primers*. 2017;3:17018. doi:10.1038/nrdp.2017.18
3. Bradbury EJ, Burnside ER. Moving beyond the glial scar for spinal cord repair. *Nat Commun*. 2019;10:3879. doi:10.1038/s41467-019-11707-7
4. Bloom O, Herman PE, Spungen AM. Systemic inflammation in traumatic spinal cord injury. *Exp Neurol*. 2020;325:113143. doi:10.1016/j.expneurol.2019.113143
5. Hellenbrand DJ, Quinn CM, Piper ZJ, Morehouse CN, Fixel JA, Hanna AS. Inflammation after spinal cord injury: a review of the critical timeline of signaling cues and cellular infiltration. *J Neuroinflammation*. 2021;18:284. doi:10.1186/s12974-021-02337-2
6. David S, Kroner A. Repertoire of microglial and macrophage responses after spinal cord injury. *Nat Rev Neurosci*. 2011;12(7):388–399. doi:10.1038/nrn3053
7. Patani R, Hardingham GE, Liddelow SA. Functional roles of reactive astrocytes in neuroinflammation and neurodegeneration. *Nat Rev Neurol*. 2023;19:395–409. doi:10.1038/s41582-023-00822-1
8. Colombo E, Farina C. Astrocytes: key regulators of neuroinflammation. *Trends Immunol*. 2016;37:608–620. doi:10.1016/j.it.2016.06.006
9. Li H, He B, Zhang X, et al. D-dopachrome tautomerase drives astroglial inflammation via NF-kappaB signaling following spinal cord injury. *Cell Biosci*. 2022;12:128. doi:10.1186/s13578-022-00867-7
10. Ji H, Zhang Y, Chen C, et al. D-dopachrome tautomerase activates COX2/PGE(2) pathway of astrocytes to mediate inflammation following spinal cord injury. *J Neuroinflammation*. 2021;18:130. doi:10.1186/s12974-021-02186-z
11. Song H, Song T, Yang T, et al. High mobility group box 1 mediates inflammatory response of astrocytes via cyclooxygenase 2/prostaglandin E2 signaling following spinal cord injury. *Neural Regen Res*. 2021;16:1848–1855. doi:10.4103/1673-5374.303039
12. Kinsella S, Fichtner M, Watters O, König HG, Prehn JHM. Increased A20-E3 ubiquitin ligase interactions in Bid-deficient glia attenuate TLR3- and TLR4-induced inflammation. *J Neuroinflammation*. 2018;15:130. doi:10.1186/s12974-018-1143-3
13. Xu J, Ji T, Li G, et al. Lactate attenuates astrocytic inflammation by inhibiting ubiquitination and degradation of NDRG2 under oxygen-glucose deprivation conditions. *J Neuroinflammation*. 2022;19:314. doi:10.1186/s12974-022-02678-6
14. Brambilla R, Bracchi-Ricard V, Hu WH, et al. Inhibition of astroglial nuclear factor kappaB reduces inflammation and improves functional recovery after spinal cord injury. *J Exp Med*. 2005;202:145–156. doi:10.1084/jem.20041918
15. Brambilla R, Hurtado A, Persaud T, et al. Transgenic inhibition of astroglial NF-kappa B leads to increased axonal sparing and sprouting following spinal cord injury. *J Neurochem*. 2009;110:765–778. doi:10.1111/j.1471-4159.2009.06190.x
16. Shembade N, Ma A, Harhaj EW. Inhibition of NF-kappaB signaling by A20 through disruption of ubiquitin enzyme complexes. *Science*. 2010;327:1135–1139. doi:10.1126/science.1182364
17. Wertz IE, O'Rourke KM, Zhou H, et al. De-ubiquitination and ubiquitin ligase domains of A20 downregulate NF-kappaB signalling. *Nature*. 2004;430:694–699. doi:10.1038/nature02794
18. Ruan J, Schluter D, Wang X. Deubiquitinating enzymes (DUBs): doUBle-edged swords in CNS autoimmunity. *J Neuroinflammation*. 2020;17:102. doi:10.1186/s12974-020-01783-8
19. Daston MM, Ratner N. Amphoterin (P30, HMG-1) and RIP are early markers of oligodendrocytes in the developing rat spinal cord. *J Neurocytol*. 1994;23:323–332. doi:10.1007/BF01188500
20. Basters A, Geurink PP, Röcker A, et al. Structural basis of the specificity of USP18 toward ISG15. *Nat Struct Mol Biol*. 2017;24:270–278. doi:10.1038/nsmb.3371
21. Ketscher L, Hannß R, Morales DJ, et al. Selective inactivation of USP18 isopeptidase activity in vivo enhances ISG15 conjugation and viral resistance. *Proc Natl Acad Sci U S A*. 2015;112:1577–1582. doi:10.1073/pnas.1412881112
22. Held T, Basler M, Knobeloch KP, Groettrup M. Evidence for an involvement of the ubiquitin-like modifier ISG15 in MHC class I antigen presentation. *Eur J Immunol*. 2021;51:138–150. doi:10.1002/eji.202048646
23. Durfee LA, Lyon N, Seo K, Huibregtse JM. The ISG15 conjugation system broadly targets newly synthesized proteins: implications for the antiviral function of ISG15. *Mol Cell*. 2010;38:722–732. doi:10.1016/j.molcel.2010.05.002
24. Park JM, Yang SW, Yu KR, et al. Modification of PCNA by ISG15 plays a crucial role in termination of error-prone translesion DNA synthesis. *Mol Cell*. 2014;54:626–638. doi:10.1016/j.molcel.2014.03.031
25. Munnur D, Teo Q, Eggermont D, et al. Altered ISGylation drives aberrant macrophage-dependent immune responses during SARS-CoV-2 infection. *Nat Immunol*. 2021;22:1416–1427. doi:10.1038/s41590-021-01035-8
26. Arimoto KI, Löchte S, Stoner SA, et al. STAT2 is an essential adaptor in USP18-mediated suppression of type I interferon signaling. *Nat Struct Mol Biol*. 2017;24:279–289. doi:10.1038/nsmb.3378
27. Zhang X, Cheng L, Gao C, et al. Androgen signaling contributes to sex differences in cancer by inhibiting nf-κb activation in t cells and suppressing antitumor immunity. *Cancer Res*. 2023;83:906–921. doi:10.1158/0008-5472.CAN-22-2405
28. Song C, Peng J, Wei Y, et al. USP18 promotes tumor metastasis in esophageal squamous cell carcinomas via deubiquitinating ZEB1. *Exp Cell Res*. 2021;409:112884. doi:10.1016/j.yexcr.2021.112884
29. Olie CS, Pinto-Fernández A, Damianou A, et al. USP18 is an essential regulator of muscle cell differentiation and maturation. *Cell Death Dis*. 2023;14:231. doi:10.1038/s41419-023-05725-z
30. Kang JA, Jeon YJ. Emerging roles of USP18: from biology to pathophysiology. *Int J Mol Sci*. 2020;21:6825. doi:10.3390/ijms21186825
31. Liu X, Li H, Zhong B, et al. USP18 inhibits NF-κB and NFAT activation during Th17 differentiation by deubiquitinating the TAK1-TAB1 complex. *J Exp Med*. 2013;210:1575–1590. doi:10.1084/jem.20122327
32. Malhotra S, Morcillo-Suárez C, Nurtdinov R, et al. Roles of the ubiquitin peptidase USP18 in multiple sclerosis and the response to interferon-β treatment. *Eur J Neurol*. 2013;20:1390–1397. doi:10.1111/ene.12193

33. Goldmann T, Zeller N, Raasch J, et al. USP18 lack in microglia causes destructive interferonopathy of the mouse brain. *EMBO J*. 2015;34:1612–1629. doi:10.15252/embj.201490791
34. Liu W, Ge X, Zhou Z, et al. Deubiquitinase USP18 regulates reactive astrogliosis by stabilizing SOX9. *Glia*. 2021;69:1782–1798. doi:10.1002/glia.23992
35. Yuan L, Xu J, Qin F, et al. USP18 overexpression protects against spinal cord ischemia/reperfusion injury via regulating autophagy. *Neurosci Lett*. 2023;810:137359. doi:10.1016/j.neulet.2023.137359
36. Francois-Newton V, Magno de Freitas Almeida G, Payelle-Brogard B, et al. USP18-based negative feedback control is induced by type I and type III interferons and specifically inactivates interferon alpha response. *PLoS One*. 2011;6:e22200. doi:10.1371/journal.pone.0022200
37. Malakhov MP, Malakhova OA, Kim KI, Ritchie KJ, Zhang DE. UBP43 (USP18) specifically removes ISG15 from conjugated proteins. *J Biol Chem*. 2002;277:9976–9981. doi:10.1074/jbc.M109078200
38. MacParland SA, Ma XZ, Chen L, et al. Lipopolysaccharide and tumor necrosis factor alpha inhibit interferon signaling in hepatocytes by increasing ubiquitin-like protease 18 (USP18) expression. *J Virol*. 2016;90:5549–5560. doi:10.1128/JVI.02557-15
39. Kim KI, Malakhova OA, Hoebe K, Yan M, Beutler B, Zhang DE. Enhanced antibacterial potential in UBP43-deficient mice against Salmonella typhimurium infection by up-regulating type I IFN signaling. *J Immunol*. 2005;175:847–854. doi:10.4049/jimmunol.175.2.847
40. Colonne PM, Sahni A, Sahni SK. Suppressor of cytokine signalling protein SOCS1 and UBP43 regulate the expression of type I interferon-stimulated genes in human microvascular endothelial cells infected with Rickettsia conorii. *J Med Microbiol*. 2013;62:968–979. doi:10.1099/jmm.0.054502-0
41. Dieterich C, Relman DA. Modulation of the host interferon response and ISGylation pathway by B. pertussis filamentous hemagglutinin. *PLoS One*. 2011;6:e27535. doi:10.1371/journal.pone.0027535
42. Song S, Xiao Z, Dekker FJ, Poelarends GJ, Melgert BN. Macrophage migration inhibitory factor family proteins are multitasking cytokines in tissue injury. *Cell Mol Life Sci*. 2022;79:105. doi:10.1007/s00018-021-04038-8
43. Illescas O, Pacheco-Fernandez T, Laclette JP, Rodriguez T, Rodriguez-Sosa M. Immune modulation by the macrophage migration inhibitory factor (MIF) family: d-dopachrome tautomerase (DDT) is not (always) a backup system. *Cytokine*. 2020;133:155121. doi:10.1016/j.cyto.2020.155121
44. Zhang M, Aman P, Grubb A, et al. Cloning and sequencing of a cDNA encoding rat D-dopachrome tautomerase. *FEBS Lett*. 1995;373:203–206. doi:10.1016/0014-5793(95)01041-C
45. Ma Y, Su KN, Pfau D, et al. Cardiomyocyte d-dopachrome tautomerase protects against heart failure. *JCI Insight*. 2019;4. doi:10.1172/jci.insight.128900
46. Kim BS, Tilstam PV, Hwang SS, et al. D-dopachrome tautomerase in adipose tissue inflammation and wound repair. *J Cell Mol Med*. 2017;21:35–45. doi:10.1111/jcmm.12936
47. Merk M, Mitchell RA, Endres S, Bucala R. D-dopachrome tautomerase (D-DT or MIF-2): doubling the MIF cytokine family. *Cytokine*. 2012;59:10–17. doi:10.1016/j.cyto.2012.03.014
48. Meza-Romero R, Benedek G, Jordan K, et al. Modeling of both shared and distinct interactions between MIF and its homologue D-DT with their common receptor CD74. *Cytokine*. 2016;88:62–70. doi:10.1016/j.cyto.2016.08.024
49. Merk M, Zierow S, Leng L, et al. The D-dopachrome tautomerase (DDT) gene product is a cytokine and functional homolog of macrophage migration inhibitory factor (MIF). *Proc Natl Acad Sci U S A*. 2011;108:E577–585. doi:10.1073/pnas.1102941108
50. Jiang Z, Shen J, Ding J, et al. USP18 mitigates lipopolysaccharide-induced oxidative stress and inflammation in human pulmonary microvascular endothelial cells through the TLR4/NF-κB/ROS signaling. *Toxicol Vitro*. 2021;75:105181. doi:10.1016/j.tiv.2021.105181
51. Hu B, Ge C, Zhu C. Ubiquitin-specific peptidase 18 negatively regulates and inhibits lipopolysaccharide-induced sepsis by targeting transforming growth factor-β-activated kinase 1 activity. *Int Immunol*. 2021;33:461–468. doi:10.1093/intimm/dxab029
52. Scheff SW, Rabchevsky AG, Fugaccia I, Main JA, Lumpp JE Jr. Experimental modeling of spinal cord injury: characterization of a force-defined injury device. *J Neurotrauma*. 2003;20:179–193. doi:10.1089/08977150360547099
53. Zhou Y, Guo W, Zhu Z, et al. Macrophage migration inhibitory factor facilitates production of CCL5 in astrocytes following rat spinal cord injury. *J Neuroinflammation*. 2018;15:253. doi:10.1186/s12974-018-1297-z
54. Basso DM, Beattie MS, Bresnahan JC. A sensitive and reliable locomotor rating scale for open field testing in rats. *J Neurotrauma*. 1995;12:1–21. doi:10.1089/neu.1995.12.1
55. Liddelow SA, Barres B. Reactive astrocytes: production, function, and therapeutic potential. *Immunity*. 2017;46:957–967. doi:10.1016/j.immuni.2017.06.006
56. Radulovic M, Yoon H, Wu JM, Mustafa K, Scarisbrick IA. Targeting the thrombin receptor modulates inflammation and astrogliosis to improve recovery after spinal cord injury. *Neurobiol Dis*. 2016;93:226–242. doi:10.1016/j.nbd.2016.04.010
57. Pasupuleti V, Du WN, Gupta Y, et al. Dysregulated D-dopachrome tautomerase, a hypoxia-inducible factor-dependent gene, cooperates with macrophage migration inhibitory factor in renal tumorigenesis. *J Biol Chem*. 2014;289:3713–3723. doi:10.1074/jbc.M113.500694
58. Pohl J, Hendgen-Cotta UB, Stock P, Luedike P, Rassaf T. Elevated MIF-2 levels predict mortality in critically ill patients. *J Crit Care*. 2017;40:52–57. doi:10.1016/j.jcrc.2017.03.012
59. Yang T, Jiang H, Luo X, et al. Thrombin acts as inducer of proinflammatory macrophage migration inhibitory factor in astrocytes following rat spinal cord injury. *J Neuroinflammation*. 2022;19:120. doi:10.1186/s12974-022-02488-w
60. Zhang H, Hu YM, Wang YJ, et al. Macrophage migration inhibitory factor facilitates astrocytic production of the CCL2 chemokine following spinal cord injury. *Neural Regen Res*. 2023;18(8):1802–1808. doi:10.4103/1673-5374.363184
61. Bernhagen J, Krohn R, Lue H, et al. MIF is a noncognate ligand of CXC chemokine receptors in inflammatory and atherogenic cell recruitment. *Nat Med*. 2007;13:587–596.
62. Schindler L, Dickerhof N, Hampton MB, Bernhagen J. Post-translational regulation of macrophage migration inhibitory factor: basis for functional fine-tuning. *Redox Biol*. 2018;15:135–142. doi:10.1016/j.redox.2017.11.028
63. Zheng Y, Li X, Qian X, et al. Secreted and O-GlcNAcylated MIF binds to the human EGF receptor and inhibits its activation. *Nat Cell Biol*. 2015;17:1348–1355. doi:10.1038/ncb3222
64. Ishimoto K, Iwata T, Taniguchi H, Mizusawa N, Tanaka E, Yoshimoto K. D-Dopachrome tautomerase promotes IL-6 expression and inhibits adipogenesis in preadipocytes. *Cytokine*. 2012;60:772–777. doi:10.1016/j.cyto.2012.07.037

65. Iwata T, Taniguchi H, Kuwajima M, et al. The action of d-dopachrome tautomerase as an adipokine in adipocyte lipid metabolism. *PLoS One*. 2012;7:e33402. doi:10.1371/journal.pone.0033402
66. Giovannoni F, Quintana FJ. The role of astrocytes in CNS inflammation. *Trends Immunol*. 2020;41:805–819. doi:10.1016/j.it.2020.07.007
67. Roy Choudhury G, Ryou MG, Poteet E, et al. Involvement of p38 MAPK in reactive astrogliosis induced by ischemic stroke. *Brain Res*. 2014;1551:45–58. doi:10.1016/j.brainres.2014.01.013
68. Rothhammer V, Mascanfroni ID, Bunse L, et al. Type I interferons and microbial metabolites of tryptophan modulate astrocyte activity and central nervous system inflammation via the aryl hydrocarbon receptor. *Nat Med*. 2016;22:586. doi:10.1038/nm.4106
69. Yeste A, Takenaka MC, Mascanfroni ID, et al. Tolerogenic nanoparticles inhibit T cell-mediated autoimmunity through SOCS2. *Sci Signal*. 2016;9. doi:10.1126/scisignal.aad0612
70. Wang X, Deckert M, Xuan NT, et al. Astrocytic A20 ameliorates experimental autoimmune encephalomyelitis by inhibiting NF-kappa B- and STAT1-dependent chemokine production in astrocytes. *Acta Neuropathol*. 2013;126:711–724. doi:10.1007/s00401-013-1183-9
71. Potu H, Sgorbissa A, Brancolini C. Identification of USP18 as an important regulator of the susceptibility to IFN-alpha and drug-induced apoptosis. *Cancer Res*. 2010;70:655–665. doi:10.1158/0008-5472.CAN-09-1942
72. Ritchie KJ, Hahn CS, Kim KI, et al. Role of ISG15 protease UBP43 (USP18) in innate immunity to viral infection. *Nat Med*. 2004;10:1374–1378. doi:10.1038/nm1133
73. Knobeloch KP, Utermohlen O, Kisser A, Prinz M, Horak I. Reexamination of the role of ubiquitin-like modifier ISG15 in the phenotype of UBP43-deficient mice. *Mol Cell Biol*. 2005;25:11030–11034. doi:10.1128/MCB.25.24.11030-11034.2005
74. Nayak TKS, Alamuru-Yellapragada NP, Parsa KVL. Deubiquitinase USP12 promotes LPS induced macrophage responses through inhibition of I kappa B alpha. *Biochem Biophys Res Commun*. 2017;483:69–74. doi:10.1016/j.bbrc.2017.01.004